Orientation of core-shell nanoparticles in an electric field

Jonghyun Park and Wei Lu[a)]
Department of Mechanical Engineering, University of Michigan, Ann Arbor, Michigan 48109

(Received 11 June 2007; accepted 6 July 2007; published online 1 August 2007)

Coated nanoparticles, which have a core-shell structure, have many applications. This letter investigates the induced torque and orientation of such nanoparticles in an electric field. The authors show that the shell of a nanoparticle has an important effect on its orientation, even when the shell is thin and takes only a small portion of the total volume. For lossy dielectric particles, the permittivity, conductivity, field frequency, and core-shell structure together determine the magnitude and direction of the induced torque, suggesting a significant degree of experimental control over nanoparticle rotation and alignment. © *2007 American Institute of Physics*.
[DOI: 10.1063/1.2767191]

The dispersion of functionalized nanoparticles with surface coatings in a dielectric medium has a wide spectrum of applications from advanced materials to nanodevices.[1] Morphology control is a key to achieving the full potential. Materials with designed distribution and orientation of nanoparticles offer superior properties, unique functionalities, and maximum flexibilities that cannot be achieved by the current uniformly/randomly dispersed nanocomposites.

Recent studies have shown that nanoparticles with anisotropic geometries may rotate preferentially under applied electric fields,[2–4] suggesting an approach to bring about controlled particle orientations in a matrix. The observations pose interesting scientific problems and call for a quantitative understanding of the phenomena. The rotation of a micro or larger sized particle in an electric field has been investigated by many researches. For instance, Saito and co-workers[5,6] were among the first to calculate the potential energy of a lossless dielectric particle and determined the stable orientation that corresponded to the lowest potential state of the system. However, nanoparticles possess several unique aspects that distinguish their behaviors from microscale counterparts. Firstly, nanoparticles are often coated with a functional layer to enhance their dispersion or to achieve specific bonding properties. This shell of coating may dominate due to the high surface-to-volume ratio and thus completely change the picture of particle orientation in response to an external field. Secondly, the effect of Brownian motion becomes important due to the small particle sizes. This letter presents rigorous calculations of the torque on core-shell nanoparticles with anisotropic geometries under an applied electric field. We show that particle structure and applied field can lead to rich behaviors and significant degree of experimental control over particle orientation. The study also reveals the competition between rotational alignment due to the electric field and randomization due to the rotational Brownian motion.

The following picture illustrates the mechanism of particle rotation. Imagine a dielectric nanoparticle in a fluidic medium. An applied electric field will induce dipole moments inside the particle. Generally speaking, when the particle has an anisotropic geometry, the direction of the total induced dipole does not coincide with that of the applied field. Thus the dipole moment interacts with the field and causes the particle to rotate. To rigorously calculate the torque on a core-shell nanoparticle, we propose a Maxwell stress tensor approach. The Maxwell stress tensor is defined by $\mathbf{S}=\varepsilon_m(\mathbf{EE}-1/2|\mathbf{E}|^2\mathbf{I})$, where $\mathbf{E}$ is the electric field, ε_m the permittivity of the medium, and $\mathbf{I}$ the identity tensor.[7] The electric torque is obtained by an area integration over a closed surface which surrounds the particle, namely,

$$\mathbf{T}_e = \int_A \mathbf{r} \times (\mathbf{S} \cdot \mathbf{n}) dA, \tag{1}$$

where $\mathbf{r}$ is a position vector and $\mathbf{n}$ is the unit normal vector of the closed surface.

Consider a confocal core-shell ellipsoid shown in Fig. 1(a), which can represent a wide range of shapes from disks to rods. The principal semiaxes are a_c, b_c, and c_c for the core surface and a_s, b_s, and c_s for the outer shell surface. Any confocal ellipsoidal surface can be expressed by $x^2/(a_s^2+u)+y^2/(b_s^2+u)+z^2/(c_s^2+u)=1 \quad (a_s>b_s>c_s)$. This equation, a cubic in u, has three real roots ξ, η, and ζ that define the ellipsoidal coordinates. The coordinate ξ is normal to the surface. In other words, each ellipsoidal surface is defined by a constant ξ. Define $\xi_c \equiv a_s^2-a_c^2=b_s^2-b_c^2=c_s^2-c_c^2$. Note that $\xi=0$ on the outer shell surface. Thus, the shell occupies the space of $-\xi_c \leqslant \xi \leqslant 0$. The electric field can be solved analytically using Laplace's equation and ellipsoidal coordinates. Consider a uniform applied field E_0 along the x direction. Theoretical analysis shows that the potentials ϕ_c in the core, ϕ_s in the shell, and ϕ_m in the medium can be expressed by

$$\phi_c = C_{cx}x,$$

$$\phi_s = C_{sx}x + D_{sx}x\int_\xi^\infty \frac{dt}{R_t(a_s^2+t)},$$

$$\phi_m = C_{mx}x + D_{mx}x\int_\xi^\infty \frac{dt}{R_t(a_s^2+t)}. \tag{2}$$

The subscripts c, s, and m denote physical quantities in the three regions of the core, of the shell, and of the medium, respectively. Here $R_t=\sqrt{(a_s^2+t)(b_s^2+t)(c_s^2+t)}$ and the con-

[a)]Author to whom correspondence should be addressed; electronic mail: weilu@umich.edu

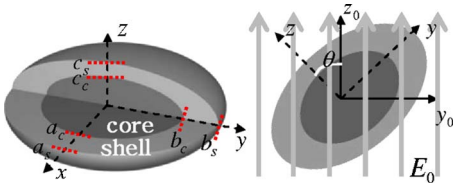

FIG. 1. (Color online) (a) Confocal core-shell ellipsoid. (b) The rotation of a core-shell particle around the x axis. The orientation is measured by the angle θ.

stants C_{cx}, C_{sx}, D_{sx}, C_{mx}, and D_{mx} are determined by the continuity and boundary conditions, i.e., the electric potentials and normal components of the electric displacements are continuous at the core-shell interface and shell-medium interface; the potential gradient at infinity must equal to the applied electric field. The continuity of the tangential electric field at the interfaces is already satisfied by Eq. (2). Similarly, we can solve the potential field when the applied field is in the y or z direction, and denote the constants with corresponding subscripts. An applied field in arbitrary directions relative to the particle axis can be treated by superposition. For an applied uniform field $\mathbf{E}_0$, we find that the electric field on the particle surface (i.e., $\xi=0$) can be expressed by

$$\mathbf{E} = \mathbf{E}_0 - \mathbf{A}\mathbf{D}_m + \frac{8\pi}{3V}\mathbf{n}(\mathbf{n}\cdot\mathbf{D}_m). \tag{3}$$

Here V is the particle volume (core plus shell), $\mathbf{A}$ is a diagonal matrix with $A_{11}=\int_0^\infty dt/(R_t\sqrt{a_s^2+t})$, $A_{22}=\int_0^\infty dt/(R_t\sqrt{b_s^2+t})$, $A_{33}=\int_0^\infty dt/(R_t\sqrt{c_s^2+t})$, and $\mathbf{D}_m=[D_{mx},D_{my},D_{mz}]^{\mathbf{T}}$.

Now consider the rotation of a lossless dielectric nanoparticle about its x axis when $\mathbf{E}_0$ is applied along the fixed z_0 axis, as shown in Fig. 1(b). The electric field in Eq. (3) is used to calculate the Maxwell stress tensor. The torque from Eq. (1) depends on the particle shape and permittivity ratios of core/medium, $\beta_c=\varepsilon_c/\varepsilon_m$ and shell/medium, $\beta_s=\varepsilon_s/\varepsilon_m$. When $\beta_s=\beta_c$, i.e., the shell and core have the same dielectric property, the particle reduces to a bare particle. Figure 2 shows the results for axially symmetric particles ($a_c=b_c$) at $\theta=45^\circ$. Superposition of $\mathbf{E}_0$ along the local y and z directions gives

$$T_e = (V\varepsilon_m E_0^2)H_e(\beta_s,\beta_c)\sin\theta\cos\theta, \tag{4}$$

where $H_e(\beta_s,\beta_c)$ is a shape function. Thus, the normalized torque $T_e/(V\varepsilon_m E_0^2)$ at $\theta=45°$ is essentially $H_e/2$. In Fig. 2 the particle is a disk with $c_c/a_c=0.1$. The thin shell is given by $\xi_c/a_c^2=0.001$ or $a_s/a_c=1.0005$. A positive torque increases θ.

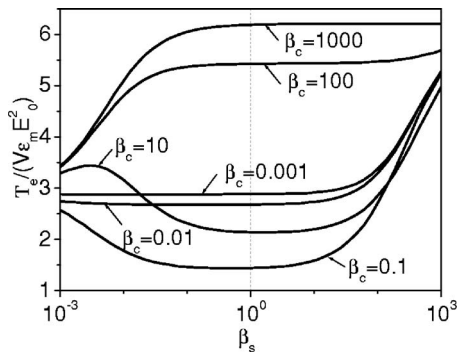

FIG. 2. Effect of shell permittivity on induced torques.

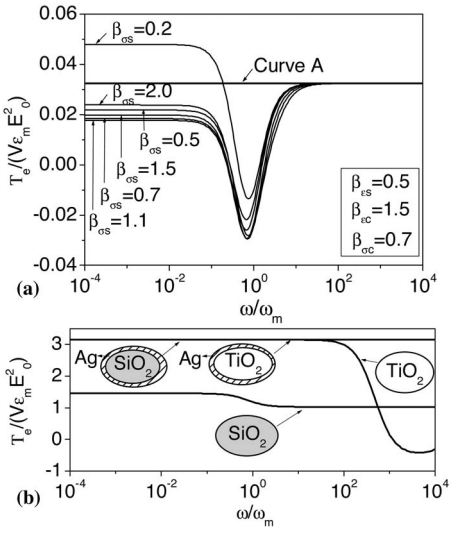

FIG. 3. (a) Effect of frequency and shell conductivity on induced torques. (b) Torques on silver-coated SiO_2 and TiO_2 nanoparticles suspended in water. We took $\varepsilon_m=80\varepsilon_0$, $\sigma_m=0.05$ S/m for water; $\varepsilon_c=3.8\varepsilon_0$, $\sigma_c=10^{-18}$ S/m for SiO_2; $\varepsilon_c=90\varepsilon_0$, $\sigma_c=300$ S/m for TiO_2; $\varepsilon_s=10\varepsilon_0$, $\sigma_s=6.3\times10^7$ S/m for the silver coating. $\varepsilon_0=8.85\times10^{-12}$ F/m.

When both the permittivities of the core and shell are larger than that of the medium ($\beta_c>1$ and $\beta_s>1$), a larger shell permittivity helps to increase the torque. In contrast, when both permittivities are smaller than that of the medium ($\beta_c<1$ and $\beta_s<1$), a smaller shell permittivity helps to increase the torque. The curves of $\beta_c=10,100,1000$ (right half, $\beta_s>1$) and $\beta_c=0.1,0.01,0.001$ (left half, $\beta_s<1$) clearly demonstrate the trend. If the core has larger and the shell has smaller permittivity than that of the medium ($\beta_c>1$, $\beta_s<1$), or vice versa ($\beta_c<1$, $\beta_s>1$), the trend becomes more complicated. The curves of $\beta_c=100,1000$ (left half, $\beta_s<1$) show that smaller shell permittivity reduces the torque. The curve of $\beta_c=10$ reaches maximum at a certain β_s when $\beta_s<1$, suggesting a competition of the core and shell contribution to the torque. The curves of $\beta_c=0.1,0.01,0.001$ (right half, $\beta_s>1$) show that larger shell permittivity increases the torque, a trend similar to those of $\beta_c>1$ curves. These diverse situations are in contrast with the simple behaviors of a bare particle ($\beta_s=\beta_c=\beta$). For a bare particle, a larger β (when $\beta>1$) or smaller β (when $\beta<1$) increases the torque.

In general, nanoparticles and the surrounding medium are not ideal dielectrics. In this case we must take into account the electric conductivity. The response of a lossy dielectric to an external field depends on the field frequency since a material's polarization does not respond instantaneously to the applied field. Define complex dielectric properties $\varepsilon_m^*(\omega)=\varepsilon_m-i\sigma_m/\omega$, $\varepsilon_s^*(\omega)=\varepsilon_s-i\sigma_s/\omega$, and $\varepsilon_c^*(\omega)=\varepsilon_c-i\sigma_c/\omega$, where ω is the frequency of the applied electric field, and σ_m, σ_s, and σ_c are the electric conductivities of the medium, shell, and core, respectively. The time-averaged Maxell stress tensor is $\mathbf{S}=1/4\,\mathrm{Re}\{\varepsilon_m\}(\mathbf{E}\mathbf{E}^*+\mathbf{E}^*\mathbf{E}-|\mathbf{E}|^2\mathbf{I})$, where $\mathbf{E}^*$ is the complex conjugate of $\mathbf{E}$.[7] The torque is still calculated by Eq. (1).

Normalize the permittivity and conductivity of the core and shell by those of the medium. Define $\beta_{\varepsilon c}=\varepsilon_c/\varepsilon_m$, $\beta_{\sigma c}=\sigma_c/\sigma_m$ for the core and $\beta_{\varepsilon s}=\varepsilon_s/\varepsilon_m$, $\beta_{\sigma s}=\sigma_s/\sigma_m$ for the shell. Note that the torque becomes frequency independent in the special case of $\beta_{\varepsilon c}=\beta_{\sigma c}$ and $\beta_{\varepsilon s}=\beta_{\sigma s}$. Figure 3 shows an

example of a core-shell disk with $c_c/a_c=0.1$. The thin shell is given by $\xi_c=0.001a_c^2$. The frequency is normalized by $\omega_m=\sigma_m/\varepsilon_m$. Note that at high frequencies the complex permittivity converges to real permittivity. Thus a particle behaves like a lossless dielectric at high frequencies. In contrast, conductivity dominates the behavior at low frequencies. Figure 3(a) clearly demonstrates the trend. The frequency-independent curve A in Fig. 3(a) has $\beta_{\varepsilon s}=\beta_{\sigma s}=0.5$ and $\beta_{\varepsilon c}=\beta_{\sigma c}=1.5$. All other curves have the same $\beta_{\varepsilon s}=0.5$, $\beta_{\varepsilon c}=1.5$ but various $\beta_{\sigma s},\beta_{\sigma c}$. They converge to flat curve A at high frequency, where conductivity has little effect on the torque. At low frequency the shell conductivity can significantly affect the torque, even though the shell takes a very small percentage of the total particle volume. These curves reveal a frequency window where the torque becomes negative. In this case the particle will rotate so that its longest axis is orthogonal to the applied field direction. At certain frequency the torque becomes zero so that a particle can stay at its current orientation. These behaviors suggest the possibility to combine material properties, core-shell structure, and field frequency to control the torque and orientation of a particle.

Figure 3(b) shows the results of silver-coated SiO_2 and TiO_2 nanoparticles suspended in water. The particles represent two situations where the permittivity and conductivity of the core is larger or smaller than that of the medium. Bare particles are considered by assigning the core permittivity and conductivity to the shell. In this way the bare and coated particles have the same volume. The highly conductive coating shields the core and dominates the torque in the shown frequency range, making the curves flat and indistinguishable of two different core situations.

To investigate the rotational dynamics of particles in a fluid, consider many axially symmetric particles ($a_c=b_c$) rotating about their x axes. The electric torque is given in Eq. (1). The rotation will be resisted by a viscous torque $-V\eta H_r\Omega$.[8] Here H_r is a shape function, η the fluid viscosity, and Ω the angular velocity. The particles undergo incessant collisions with liquid molecules. These collisions cause a random torque, which we analyze by a stochastic approach. Using an orientation distribution function (ODF) Ψ, which represents the probability of the particle being found in a specific orientation, we can express the torque for Brownian motion by $k_BT\mathbf{z}\times[\partial(\ln\Psi)/\partial\mathbf{z}]$[9], where k_B is Boltzmann's constant, T the absolute temperature, and $\mathbf{z}$ the unit orientation vector along the local z axis of a particle. Obtaining Ω from the balance of the three torques and substituting it into the continuity equation of ODF gives

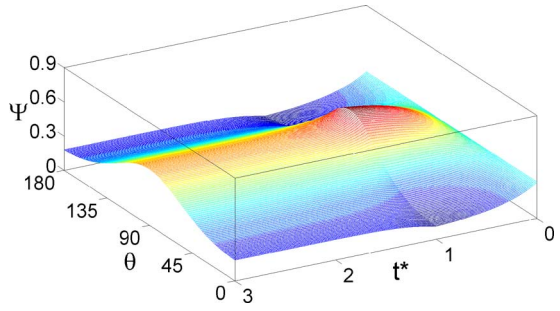

FIG. 4. (Color online) ODF evolution with $\lambda=2$ $(0\leqslant t^*\leqslant 1)$ and $\lambda=1(t^*\geqslant 1)$.

$$\frac{\partial\Psi}{\partial t^*}+\lambda\frac{\partial}{\partial\theta}(\Psi\sin 2\theta)-\frac{\partial^2\Psi}{\partial\theta^2}=0, \tag{5}$$

where $t^*=t(k_BT)/(V\eta H_r)$ is the normalized time and $\lambda=V\varepsilon_m E_0^2 H_e/(2k_BT)$. Thus two competing effects, the alignment due to the applied field and randomization due to the rotational Brownian motion, determine the evolution of Ψ. A lager λ means stronger alignment effect. We solved Eq. (5) by the Fourier spectral method. Figure 4 shows ODF evolution from an initial random distribution. Over time more particles orient close to $\theta=90°$. After reducing λ from 2 to 1 at $t^*=1$, ODF starts to relax and spread.

In summary, we proposed an approach to rigorously calculate the electric torque on a dielectric core-shell particle. The study showed that the shell has an important effect, even when it is thin and takes a small portion of the total volume. For lossy dielectrics, the core-shell structure demonstrated frequency dependent behavior and a window to tune the preferential orientation. The ODF evolution demonstrated the competition between rotational alignment due to the electric field and randomization due to the rotational Brownian motion.

The authors acknowledge financial support from National Science Foundation CAREER Award No. DMI-0348375.

[1]F. Hussain, M. Hojjati, M. Okamoto, and R. E. Gorga, J. Compos. Mater. **40**, 1511 (2006).
[2]D. L. Fan, F. Q. Zhu, R. C. Cammarata, and C. L. Chien, Appl. Phys. Lett. **89**, 223115 (2006).
[3]J. Gimsa, Biochemistry **54**, 23 (2001).
[4]V. I. Merkulov, A. V. Melechko, M. A. Guillorn, M. L. Simpson, D. H. Lowndes, J. H. Whealton, and R. J. Raridon, Appl. Phys. Lett. **80**, 4816 (2002).
[5]M. Saito, H. P. Schwan, and G. Schwarz, Biophys. J. **6**, 313 (1966).
[6]G. Schwarz, M. Saito, and H. P. Schwan, J. Chem. Phys. **43**, 3562 (1965).
[7]Xujing Wang, Xiao-Bo Wang, and Peter R. C. Gascoyne, J. Electrost. **39**, 277 (1997).
[8]J. J. Newman, and R. B. Yarbrough, J. Appl. Phys. **39**, 5566 (1968).
[9]R. B. Bird, R. C. Armstrong, and O. Hassager, *Dynamics of Polymeric Liquid* (Wiley, New York, 1977).